Journal of Coastal Research	SI 56	pg - pg	ICS2009 (Proceedings)	Portugal	ISSN

Macrotidal rip current experiment: circulation and dynamics

M. J. Austin†, T. M. Scott†, J.W. Brown‡, J.A. Brown‡ and J. H. MacMahan∞

†School of Earth, Ocean and Environmental Sciences, University of Plymouth, Plymouth, PL4 8AA, UK
martin.austin@plymouth.ac.uk; timothy.scott@plymouth.ac.uk

‡ Civil and Environmental Engineering, University of Delaware, Newark, DE, USA
jwbrown@udel.edu; brownja@udel.edu

∞ Navel Postgraduate School, Oceanography Department, Monterey, CA, 93942, USA
jhmacmah@nps.edu

ABSTRACT

AUSTIN, M. J., SCOTT, T. M., BROWN, J. W., BROWN, J. A. and MACMAHAN, J. H., 2009. Macrotidal rip current experiment: circulation and dynamics. Journal of Coastal Research, SI 56 (Proceedings of the 10th International Coastal Symposium), pg – pg. Lisbon, Portugal, ISBN

The macrotidal intermediate–dissipative beaches of the southwest UK display strong seasonality whereby extensive low-tide bar/rip systems form during the spring season. These features reach a state of maximum development during the summer months, when strong rip currents are present at various stages of the tide that switch on/off due to tidal translation. This research investigates for the first time the circulation and dynamics of macrotidal rip systems from the perspective of the flow dynamics and surf zone circulation. A field experiment was conducted on a macro-tidal beach (range 6.3 m) with low-tide bar/rip morphology to quantify the circulation and dynamics of the rip current systems. Measurements of flow velocity, water depth and suspended sediment concentration were collected over the channel and shoal of a transverse bar/rip system using an in-situ sensor array, whilst the surf zone circulation patterns were monitored with post-processed GPS drifter floats. The in-situ data show that currents within the rip system are strongly correlated with the stage of the tide and maximum current speeds are recorded during the 3-hour period immediately around low water. During this period, wave breaking is maximised on the adjacent shoal resulting in a longshore gradient in wave dissipation. The GPS drifters indicate that an extensive rotational surf zone circulation pattern exists, whereby the offshore flow within the rip channel returns landwards over the intertidal bar from the outer edge of the surf zone.

ADITIONAL INDEX WORDS: *Surf zone, Nearshore circulation, Wave breaking, Morphodynamics*

INTRODUCTION

Rip currents are an integral component of nearshore cell-circulation, returning water seawards from within the surf zone as a confined energetic jet. This has significant implications from the perspective of beach safety and life-guarding, where rip currents present a serious hazard to beach users. Rip currents are known to be modulated by tidally-induced changes in water level and the macrotidal nature of many beaches in the Southwest UK provides the ideal setting in which to examine this modulation.

Rip currents are most often observed when the waves approach at near shore-normal incidence and where there are alongshore variations in bathymetry and incised sandbars. The pre-existence of template morphology on the beachface will therefore act to focus the alongshore gradients in radiation stress. Waves will break over nearshore sandbars, with a corresponding increase in radiation stress to landwards; however, waves will not break over the incised channels so an alongshore gradient in radiation stress will develop in the lee of the bar. In the classic scenario, an alongshore current will flow from landwards of the bar (feeder channel), before turning seawards and exiting the surf zone as a rip.

While rip currents are forced by the incoming wave energy, they may be strongly influenced by tidal elevation (e.g. AAGAARD *et al*., 1997; BRANDER and SHORT, 2001). The tide may modulate rip currents such that decreases in tidal elevation increase rip current flows to a relative maximum (AAGAARD *et al*., 1997; BRANDER and SHORT, 1999; MACMAHAN *et al*., 2005), and the presence and danger of rip currents are frequently linked to lower tidal stages. The switching on and off and the apparent alongshore movement of rips as the tide translates through mid-, low- and mid-tide increases the temporal beachface hazard signature and could be a key driver in 'mass rescue events' occurring on certain beaches (refer to SCOTT *et al*., this issue).

It would be expected that topographic confinement of rip flow would be enhanced at low tide (BRANDER and SHORT, 2001), but this raises the question as to whether morphological control is manifest by distinct flow channelisation or by the enhancement of set-up gradients caused by wave dissipation over varying morphology. SONU (1972) states that wave breaking over nearshore bars is essential to the formation of rip circulation and that the intensity of breaking, controlled by the tide, corresponds to a proportionally stronger circulation. However, the findings of BRANDER and SHORT (2001) provide some support for the idea of morphologic flow constriction with the observation that narrow rip channels with pronounced banks were more sensitive to tidally-induced water depth changes. SHORT (1985) hypothesizes that flow velocity is stable whilst constrained within the channel, but that once the banks are overtopped with increasing water depth the flow dramatically reduces.

Perhaps more importantly, tidally induced changes in water depth modify the interaction of incident waves and existing morphology. The presence of transverse or significantly incised

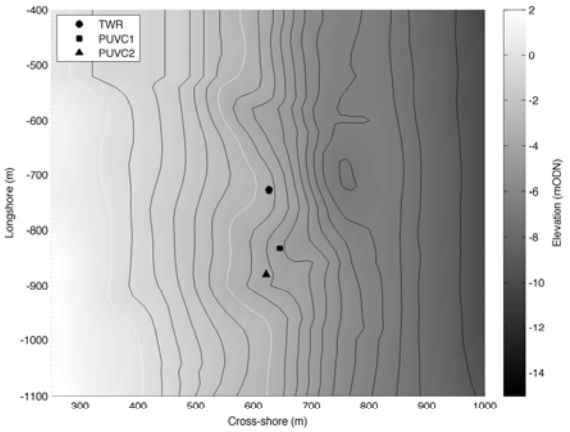

Figure 1. Combined results of the intertidal RTK-GPS survey and nearshore bathymetry indicating the instrument positions. Shading and contours indicate water depth (mODN; Ordnance Datum Newlyn). White contours indicate the mean low water spring (-3 m) and mean sea level (0 m).

shore parallel sandbars in the intertidal/nearshore zone affect wave breaking and changes in water depth create a temporal pattern of wave breaking over these bars. Suppose two transverse bars are located low on the intertidal beachface and are separated by a single shore normal channel. At high- and mid-tide the proportion of waves breaking over the bars will be small and hence there will be little in the way of an alongshore gradient in set-up. As the water level falls, wave breaking increases over the bar crests and an alongshore set-up gradient is established. Water flows alongshore landwards of the bars, converging at the landwards end of the channel before flowing seawards; the rip current is now 'working'. Therefore at some critical water depth over the bar, the set-up gradient and hence rip current flow will be maximised.

METHODOLOGY

A 10-day field experiment was conducted at Perranporth, Cornwall, UK during August 2008. Perranporth is a macrotidal beach with a mean spring tide range of 6.3 m and it falls at the transition between the low tide bar/rip and dissipative morphological states. Regular intertidal beachface surveys were carried out using a real-time kinematic global positioning system (RTK-GPS) mounted on an all-terrain vehicle (ATV) and a bathymetric survey was conducted during the experiment.

The morphology during the field experiment was characterised by extensive bar/rip systems located around the low water level (-3 m) and a sub-tidal bar located in 7 m water depth. The incised rip channels were quasi-periodic with a spacing O(400 m) (Figure 1).

Rip current dynamics were monitored using a small array of current meters and pressure transducers (PT). Flow dynamics within a rip channel and adjacent incised shore-parallel low-tide bar/feeder region were measured with Nortek Vector 3D-ADV's equipped with an external PT, OBS and battery pack (PUVC). The head of the ADV's and co-located sensors were mounted 0.2 m above the bed. An RBR TWR2050 PT (TWR) located on the crest of the intertidal bar recorded water depth for 8.5-min bursts every 10 min. All instruments were sampled synchronously and logged

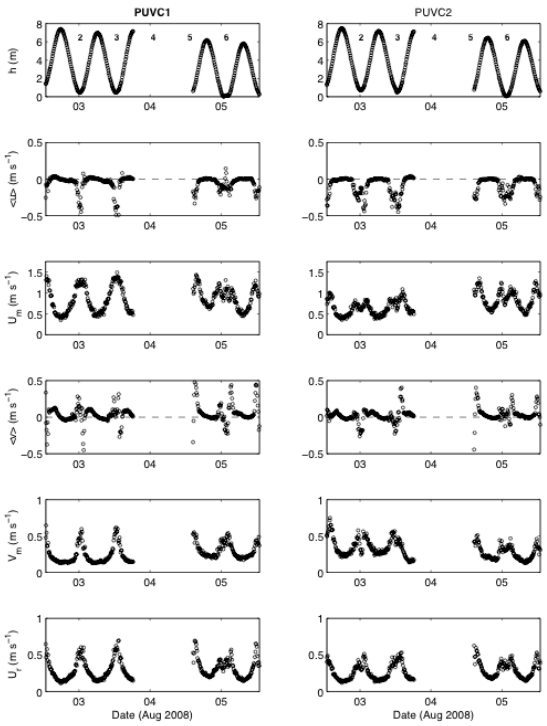

Figure 2. Summary of the flow statistics measured by the in-situ instruments at 10-min intervals for the feeder (PUVC1) and rip (PUVC2) locations. (From top) Water depth h; mean cross-shore flow velocity $\langle u \rangle$, positive onshore; maximum cross-shore orbital velocity U_m; mean longshore flow velocity $\langle v \rangle$, positive north; maximum longshore orbital velocity V_m; and U_r mean return speed. Numbers in the upper panel indicate the low tide number. LT4 is missing due to an instrument failure.

at 4 Hz. Offshore waves were measured by a directional waverider buoy (DWR) moored in 10 m water depth.

Rip drifter floats were constructed following a design similar to SCHMIT *et al.* (2003) and their position was monitored at 0.5 Hz using GPS loggers that were post-processed from a static base position following MACMAHAN *et al.* (2009). Drifters were released into the surf zone in clusters of 4 and allowed to circulate with the currents until they either grounded at the shoreline or escaped from pre-defined longshore and offshore boundaries. The drifter positions were transformed to local cross- and longshore coordinates and velocities.

RESULTS

Tide and wave climate

The experiment was conducted over the peak spring tide period and tidal ranges were in excess of 5.5 m. Significant wave height and peak period were 1–2 m and 7–12 s, respectively and were similar at both offshore and inshore locations, which is indicative of swell conditions. During tide 4–5, T_p reduced sharply as strong NW winds caused local wave generation. The mean wave direction was -19° (left of shore normal), except for during periods

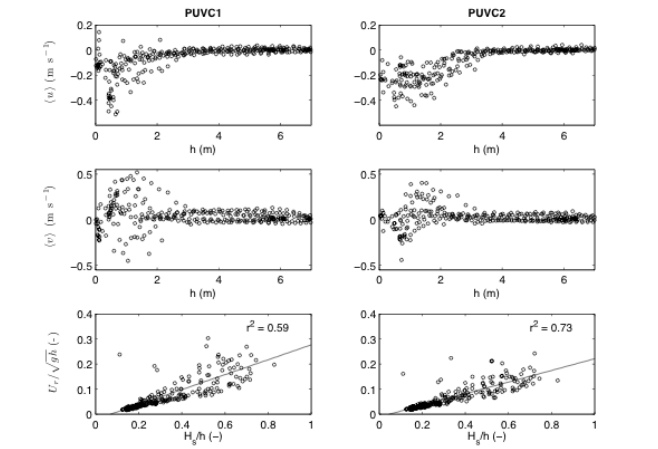

Figure 3. Scatter plots of (top) mean cross-shore current and (middle) mean longshore current vs. water depth; and (bottom) Froude number vs. relative wave height on the bar crest indicating linear fit.

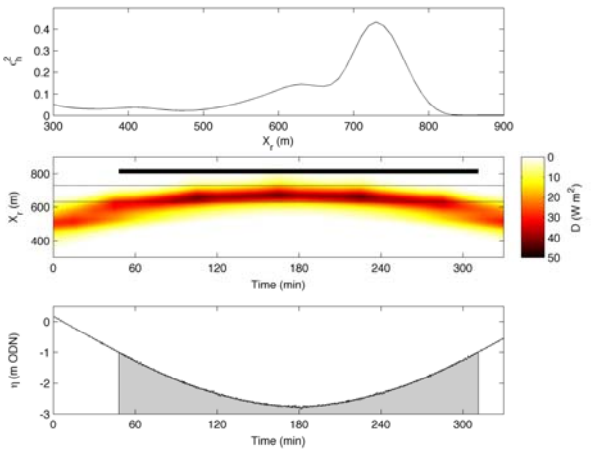

Figure 4. Modelled cross-shore distribution of wave energy dissipation. (top) Cross-shore distribution of bathymetric non-uniformity; (middle) alongshore-averaged dissipation (shading) as a function of time and indicating the locations of maximum non-uniformity (dashed lines) and the period of rip activity (black bar); and (bottom) tidal elevation where the shaded region indicates the period of rip activity.

of local wave generation when it was ~0°. Although the swell waves approached slightly oblique to the shoreline, refraction due to the local bathymetry between the DWR and the shoreline created near-normal incidence and resulted in relatively weak net longshore currents; longshore currents associated with rip circulation were present.

In-situ Eularian flow velocity

A range of statistical hydrodynamic parameters were computed from the 2048 samples (~8.53-min) collected every 10-min. The in-situ instruments were deployed below the MLWS elevation and water depth over each tide varied between 0.5 and 7 m. Summary statistics for the flow velocity data indicate significant tidal modulation of the currents with maximum flows around low water at both PUVC rigs (Figure 2). Mean cross-shore flows $\langle u \rangle$ are generally offshore and reach -0.5 m s^{-1}, whilst cross-shore orbital velocities are 0.5–1.5 m s^{-1}. Mean longshore currents $\langle v \rangle$ were recorded up to 0.5 m s^{-1} to both the north and south with maximum orbital velocities of 0.6 m s^{-1}. Due to the circulation around the bar/rip, flow was not always directed in either a cross- or longshore direction so the mean return speed U_r was computed as ($=\sqrt{u^2+v^2}$); maximum U_r coincided with the lowest tidal stages.

Rip scaling

The rip flow velocity is clearly dependant on the tidal elevation; mean cross-shore currents begin to increase in the offshore direction once a threshold depth of ~3 m is reached, and although more variable in direction, the longshore currents also increase below this threshold. Due to varying conditions on each day of the experiment, rip current speeds display some relationship with wave energy and water depth. Therefore a dimensionless rip current velocity (Froude number) was computed following HALLER *et al.* (2002) and MACMAHAN *et al.* (2005)

$$= U_r / \sqrt{gh} \qquad (1)$$

where U_r is the mean return speed, g is gravity and h the local water depth and this was observed to have a good linear relationship with the relative wave height H_s/h (which provides an indication of wave breaking) with r^2 values of 0.59 and 0.73 for PUVC1 and PUVC2, respectively (Figure 3). Note the relative wave height has been computed using the significant wave height and water depth as measured on the bar crest rather than the offshore wave height as used by MACMAHAN *et al.* (2005); however, the wave height on the bar crest and at the DWR in 10 m water depth are very similar.

An alternative scaling of the rip velocity was suggested by BRANDER and SHORT (2001) as

$$\frac{U_r}{H_s/T_p} \propto \frac{h}{h_{ht}} \qquad (2)$$

where h_{ht} is the water depth at high tide. This scaling, which normalizes the rip speed with the wave steepness, provides a similar result to the Froude scaling with the rip speed increasing significantly below $h/h_{ht} \approx 0.5$, or in other words from mid-tide, peaking at the minimum tidal elevation ($h/h_{ht} \approx 0.1$). This strong tidal dependence has previously been noted by, amongst others, AAGAARD *et al*. (1997), BRANDER and SHORT (2001), MACMAHAN *et al*. (2005), but the issue is what process drives this relationship?

Bathymetric non-uniformity

The strong linear relationship between U_r and H_s/h suggests that the modulation of wave breaking on the adjacent bars controls rip current strength (SONU, 1972) and therefore the distribution of the bathymetric variability may be the controlling factor. A measure of alongshore bathymetric non-uniformity (FEDDERSEN and GUZA, 2003) is the alongshore depth variance, $\sigma_h^2(x)$, defined as

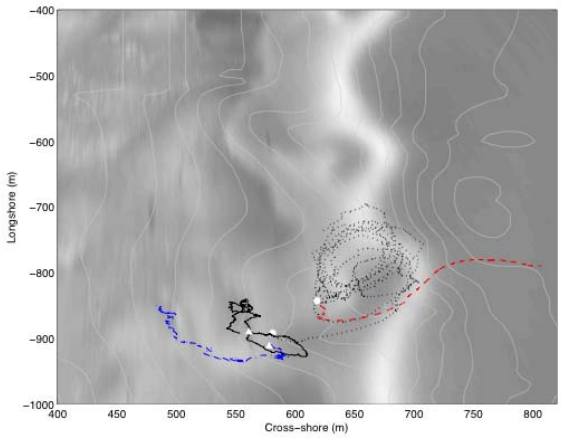

Figure 5. Drifter position and speed tracks during four deployments illustrating variable behavior: rotational circulation (dotted); escape (dash); meandering (solid); and wash up (dot-dash). Initial drifter deployment marked by white circles (LW) and triangles (LW+2.25 hr). Bathymetry is contoured in the background with the wave breaking from the Argus cameras shown as colour intensity.

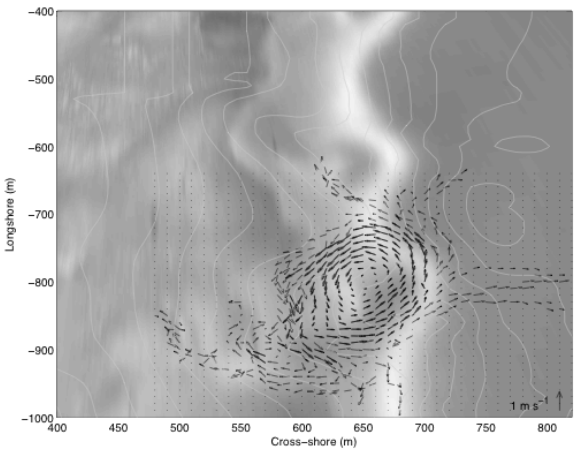

Figure 6. Drifter velocity sorted into 10m x 10 m bins and averaged over the deployment duration for bins with >5 independent observations (solid arrow) and bins with at least one observation (dashed arrow). The velocity scaling for the arrows is indicated in the lower right corner.

$$\sigma_h^2(x) = \frac{1}{L_y}\int_0^{L_y}\left[z(x,y) - \overline{z(x)}\right]^2 dy \quad (3)$$

where $z(x,y)$ is the bottom elevation, $\overline{z(x)}$ is the alongshore mean cross-shore profile, L_y is the alongshore integration distance and d_y the alongshore grid spacing. Data from the RTK surveys are used to compute $\sigma_h^2(x)$.

The distinct bar-trough morphology is clearly evident from the cross-shore variation in $\sigma_h^2(x)$ (Figure 4). There is significant alongshore variance spanning the cross-shore region at X_r = 500–830 m, with the maximum variance located at X_r = 630–730, corresponding to the incised low tide bar-trough.

Modelled cross-shore breaker dissipation

To examine the cross-shore distribution of wave breaking the wave energy dissipation was computed using the XBeach model (ROELVINK *et al.*, 2008). Dissipation was computed as the product of the total wave dissipation according to ROELVINK (1993) and the roller energy dissipation, where dissipation of wave energy serves as a source term for the roller energy balance; tide and wave conditions as observed during LT5 were used as model input.

Figure 4 shows that the cross-shore distribution of modelled energy dissipation closely matches the regions of maximum alongshore non-uniformity. The temporal variation in the dissipation shows a clear tidal dependence and for the entire period during which the rip was functioning, wave breaking occurred across the region of maximum alongshore non-uniformity; once breaking shifted landwards of this region, the rip activity ceased.

Lagrangian drifter observations

Drifter floats were deployed over the low tide period to investigate the rip current circulation across the nearshore. After deployment, drifters repeatedly migrated around the surf zone in a rip current circulation cell and/or were repeatedly re-released, providing a set of temporally evolving lagrangian observations in space.

Circulation patterns

The drifter tracks for a number of deployments displaying varying behavior during LT2 are plotted in Figure 5. The behavior includes long-term rotational circulation for a period of 1.6 hr, surf zone meandering, swash-induced wash-up and a surf zone escape. It is interesting to note that three of the drifters were deployed at approximately the same location, but with differing results. This is probably due to the change in the tidal elevation, since the two drifters that did not circulate were deployed 2.25 hr after low water when the rip speeds had significantly decreased (Figure 2) when compared to the low tide deployments that resulted in the rotational and surf zone escape rip behavior.

Mean circulation

To provide a mean description of the circulation pattern the spatial extent of the nearshore was split into 10 m x 10 m bins and the drifter observations during LT2 averaged within each bin. A drifter was considered as an independent observation when within a particular bin. If a drifter re-entered the same bin, it was considered a new independent observation if $t > l_g/U$ had elapsed, where l_g is the length of the bin and U is the average speed for all drifter observations in that bin. Bins with at least 5 independent observations were considered statistically significant.

It is clear from Figure 6 that a large rotational rip current circulation exists within the surf zone with cross- and longshore length scales of ~200 m. The rip circulation was counter-clockwise and travelled offshore through the surf zone under an angle until reaching the most seawards breaker line. The flow then turned longshore for ~75 m before returning through the surf zone over the shallow intertidal bar at [x,y] = [650m, 750m]. There were several points in the circulation pattern where drifters would at times escape the surf zone to seawards, be ejected into adjacent circulation cells or meander in very shallow water to landwards.

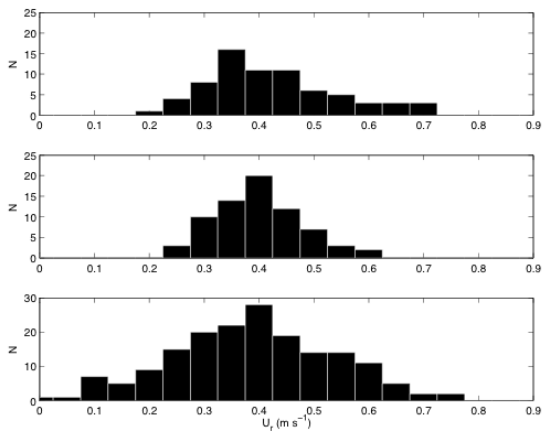

Figure 7. Comparison of Eularian and Lagrangian drifter speeds U_r. Mean rip current speed at PUVC1 (top) and PUVC2 (middle) during periods when the rip current was active (η < -1 mODN) and (bottom) rip speed from the statistically significant mean drifter circulation.

Rip current speeds

The flow speeds recorded by the Lagrangian drifters from within the rip current circulation are within the range 0.01–0.8 m s^{-1} with the maximum speeds recorded in the seaward flow through the incised channel and in the landwards directed mass flux over the bar. The modal drifter speed of 0.4 m s^{-1} is comparable with the mean rip return speeds recorded by the in-situ instrumentation (0.35–0.4 m s^{-1}), but there is a greater proportion of higher speeds (Figure 7). This is probably due to the higher number of spatial observations recorded by the drifters in the region of maximum circulation compared to the single points of current measurement.

CONCLUSIONS

The results present novel findings of rip current behavior in a macrotidal environment. In-situ sensors and GPS-tracked Lagrangian surf zone drifters have been used to quantify the rip flow dynamics and circulation over a low-tide bar/rip system.

From the present analysis of a limited number of tides, it can be identified that:

- There is significant tidal modulation of the rip current activity with the rips only active during a 3-hour period around low tide. The maximum mean Eulerian flows were recorded at low water and were directed offshore with peak velocities of -0.5 m s^{-1}. Longshore flow velocities were of the same order of magnitude and also peaked at low water.
- Rip current speed, parameterized as a Froude number, scaled well with the relative wave height on the intertidal bar crest ($r^2 \approx 0.65$). This suggests that wave breaking across the regions adjacent to the rip channels is necessary to drive the rip currents.
- Wave energy dissipation was modelled across the nearshore region using the measured tide and wave conditions. This indicated that the rip current was only active during the period when waves were breaking over the region of maximum bathymetric non-uniformity–the adjacent incised bars.
- Lagrangian drifters identified several modes of circulatory surf zone behavior during LT2: rotation, ejection, meandering and wash-up. The rotational mode was dominant with some drifters circulating for >1.5 hours.
- Spatial and temporal averaging of the independent drifter observations for the low tide period identified a significant counter-clockwise rotational surf zone circulation with cross- and longshore dimensions of ~200 m. The rip current flowed offshore through the incised rip channel before returning landwards over the shallow intertidal bar crest where the wave breaking was maximized.

Further analysis of the data collected during this field experiment will elucidate the physical processes which drive the tidal modulation of the rip currents on macrotidal beaches. The ultimate aim is to parameterize and incorporate these processes into existing 2DH numerical models and subsequently produce an end-user optimized predictive tool to aid beach hazard classification.

LITERATURE CITED

AAGAARD, T.; GREENWOOD, B., and NIELSEN, J., 1997. Mean currents and sediment transport in a rip channel. *Marine Geology*, 140(1-2), 25-45

BRANDER, R.W. and SHORT, A.D., 2001. Flow kinematics of low-energy rip current systems. *Journal of Coastal Research*, 17(2), 468-481

FEDDERSEN, F. and GUZA, R.T., 2003. Observations of nearshore circulation: Alongshore uniformity. *Journal of Geophysical Research* 108(C1), doi:10.1029/2001JC001293

HALLER, M.; DALRYMPLE, R., and SVENDESEN, I., 2002. Experimental study of nearshore dynamics on a barred beach with rip channels. *Journal of Geophysical Research*, 107, 1-21

MACMAHAN, J.H.; THORNTON, E.; STANTON, T., and RENIERS, A.H.M., 2005. RIPEX: Observations of a rip current system. *Marine Geology*, 218(1-4), 113-134

MACMAHAN, J.H.; BROWN, J., and THORNTON, E., 2009. Low-cost hand-held global positioning system for measuring surfzone currents. *Journal of Coastal Research*, in press.

ROELVINK, D., 1993. Dissipation in random wave groups incident on a beach. *Coastal Engineering*, 19, 127–150.

ROELVINK, D.; Reniers, A.; van Dongeren, A.; van Thiel de Vries, J.; Lescinski, J. and Walstra, D., 2008. Modeling hurricane impacts on beaches, dunes and barrier islands.

SCHMIT, W.B.; WOODWARD, K.; MILLIKAN, R.; GUZA, R.T.; RAUBENHEIMER, B., and ELGAR, S., 2003. A GPS-tracked surf zone drifter. *Journal of Atmospheric and Ocean Technology*, 20, 1069-1075

SCOTT, T.M.; RUSSELL, P.R.; MASSELINK, G. and WOOLER, A., 2009. Rip current variability and hazard along a macro-tidal coast. *Journal of Coastal Research*, SI 56, pg – pg

SHORT, A.D., 1985. Rip current type, spacing and persistence, Narrabeen beach, Australia. *Marine Geology*, 65, 47–71.

SONU, C.J., 1972. Field observations of nearshore circulation and meandering currents. *Journal of Geophysical Research*, 77, 3232–3247.

ACKNOWLEDGEMENTS

We would like to thank Paul Russell, Saul Reynolds, Iain Fairly, Tim Poate, Matt Hilton, Will Hibberd and James Moon for their excellent help during the field deployment.